

## Plasmons in Lithium Ammonia

C. A. Burns,<sup>1</sup> P. Abbamonte,<sup>2,3</sup> E. D. Isaacs,<sup>2</sup> and P. M. Platzman<sup>2</sup>

<sup>1</sup>*Department of Physics, Western Michigan University, Kalamazoo, Michigan 49008*

<sup>2</sup>*Bell Labs, Lucent Technologies, Murray Hill, New Jersey 07974*

<sup>3</sup>*Department of Physics, University of Illinois, 1100 W. Green Street, Urbana, Illinois 61801*

(Received 18 March 1999)

We report inelastic x-ray scattering measurements of the energy, linewidth, and dispersion of the plasmon in metallic lithium ammonia at an electron concentration of  $4 \times 10^{21} \text{ e}^-/\text{cm}^3$ . These are the first measurements of plasmons in this system, which has the lowest electronic density for which a metal plasmon has been studied. We find a plasmon whose dispersion is only slightly reduced from the RPA value, and which is quite broad with an unusual momentum dependence.

PACS numbers: 71.45.Gm, 78.70.Ck

The discovery that the alkali metals dissolve in ammonia was made over a century ago by Weyl [1]. In these systems the outermost electron dissociates from the atom, leaving a free electron and an ion. Numerous studies using a variety of techniques have helped explain the nature and properties of these systems [2]. Based on these experiments and theoretical modeling using both path integral Monte Carlo and Car-Parrinello local spin density functional methods [3], the following picture for the behavior of the solutions has emerged. At concentrations below  $10^{-3}$  mole % metal (MPM) the electrons are thought to reside in isolated cavities surrounded by polarized ammonia molecules, while at higher concentrations ( $\sim 10^{-3}$ –0.5 MPM) the electrons form closely associated pairs called bipolarons. As the concentration is increased these pairs begin to cluster together and eventually form a multitunnel structure [4]. At a concentration near 4 MPM the systems undergo a metal-insulator transition. There is a narrow range of temperatures and concentrations where the liquid phase separates into a metallic phase and an insulating phase. The system remains metallic up to the concentration limit, which is about 21 MPM for lithium.

Since the electron density in these systems is extremely low, electron-electron interactions are expected to play a large role in the electronic properties. These interactions alter the properties of electronic excitations such as the plasmon. The properties of the electron liquid at  $T = 0$  are determined by the electron density which can be described by  $r_s$  which is

$$r_s = \frac{(\frac{4}{3}\pi n)^{-1/3}}{a_0^*}, \quad (1)$$

where  $n$  is the free electron concentration and  $a_0^*$  is the effective Bohr radius,  $a_0^* = \hbar^2 \epsilon / m^* e^2$ . Here  $\epsilon$  is the static dielectric constant,  $m^*$  is the effective mass of the electron, and  $e$  is the electric charge.  $r_s$  is approximately the ratio of the Coulomb to kinetic energies for the electron in a uniform electron gas at zero temperature. Studies at large values of  $r_s$  are therefore interesting because the electron-electron interactions are more important. Typical metals have  $2 < r_s < 6$ , while for the lithium ammonia

system  $r_s$  varies from 7.35 to 11.3 for the metallic solution, and  $r_s \rightarrow \infty$  as the concentration goes to zero.

The two main experimental probes for studying the excitation spectrum as a function of momentum transfer are electron energy-loss spectroscopy (EELS) and inelastic x-ray scattering (IXS). EELS requires very thin samples with good surfaces under high vacuum, and multiple scattering effects are a significant complication. As a result, only low momentum transfers can be studied. IXS lacks such limitations but is best suited for relatively low- $Z$  materials with long x-ray absorption lengths, since the ratio of absorption length to inelastic x-ray scattering length determines the inelastic count rate. The availability of high brightness second and third generation x-ray synchrotron light sources has greatly increased the number of materials and types of studies that can be carried out with IXS [5].

In this Letter we report nonresonant inelastic x-ray scattering studies of the plasmon in the liquid metal  $\text{Li}(\text{NH}_3)_4$ . For our sample  $r_s \approx 7.35$  [assuming  $\epsilon = 1$  and the bare electron mass in Eq. (1)], which is a larger value for  $r_s$  than in any other metal and corresponds to an electron concentration of about  $4 \times 10^{21} \text{ e}^-/\text{cm}^3$ . At low momentum transfer, we see a well-defined excitation with a finite linewidth and an energy of about 2 eV. The excitation is quite broad and disperses to higher energies and broadens as the momentum transfer is increased.

Samples of lithium ammonia were made by combining 99.9% pure lithium with 99.999% pure ammonia. The electron density was determined from the amounts of lithium and ammonia added and the known density of the compound, assuming each lithium atom contributed one electron. The sample cell was a thin-walled (0.02 cm) beryllium cylinder whose diameter (0.53 cm) was approximately an absorption length for the solution. All materials used in the cell were tested and found not to react with the mixtures. Lithium was introduced into the sample cell under an argon atmosphere. A measured amount of ammonia was condensed into the sample cell at about  $-78^\circ\text{C}$ . The filled sample cell was sealed off and then placed inside a vacuum can to reduce air scatter of the x rays. The sample was kept at a temperature of  $-50^\circ\text{C}$  by

means of a three stage Peltier cooler to avoid degradation. Spectra at the beginning and end of the run were identical, indicating no alteration in the sample quality over time. The sample described here was a  $20 \pm 1$  MPM solution.

In IXS an x ray with a well-defined energy, momentum, and polarization ( $\hbar\omega_i, \hbar\mathbf{k}_i, \hat{e}_i$ ) scatters into a new state described by ( $\hbar\omega_f, \hbar\mathbf{k}_f, \hat{e}_f$ ). The energy loss of the x-ray photon is  $\hbar\omega = \hbar\omega_f - \hbar\omega_i$ , while the momentum transferred to the system is  $\mathbf{q} \equiv 2\hbar\mathbf{k}_i \sin(\theta/2)$ , where  $\theta$  is the scattering angle. Nonresonant IXS measures the scattering cross section, which is proportional to the imaginary part of the dielectric function [6]

$$\frac{d^2\sigma}{d\Omega d\omega_f} \propto q^2 \text{Im}[\varepsilon(\mathbf{q}, \omega)]^{-1}. \quad (2)$$

Collective modes such as the plasmon are related to the zeros of the real part of  $\varepsilon(\mathbf{q}, \omega)$ .

The experiment was carried out on beam line (X21) at the National Synchrotron Light Source at Brookhaven National Laboratory. The experimental setup for this beam line has been described in detail by Kao *et al.* [7]. Measurements were taken using a spherically bent, diced, germanium (733) analyzer [8] in a near backscattering geometry. The analyzer was tuned to an energy of 8977.7 eV; a Lorentzian fit to the elastic peak yielded an energy resolution for the system of 0.26 eV. Measurements were taken by scanning the incident energy and leaving the analyzer energy fixed. In the region of the plasmon we had a signal of about one count per second. All data have been normalized to the incident flux.

Figure 1 shows the inelastic x-ray scattering spectrum (at  $q = 0.4 \text{ \AA}^{-1}$ ) in the empty sample cell, in pure liquid ammonia, and in Li(NH<sub>3</sub>)<sub>4</sub>. The signal rises as the energy transfer goes to zero due to elastic and quasielastic

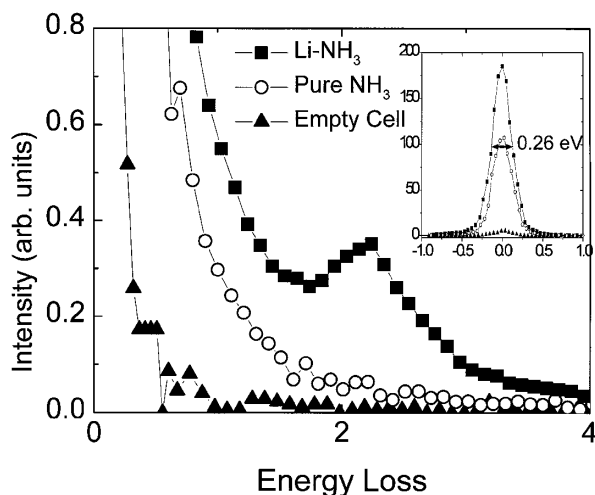


FIG. 1. Inelastic x-ray scattering signal from the empty cell, from pure ammonia, and from a 20 MPM lithium ammonia mixture. The momentum transfer here is  $0.42 \text{ \AA}^{-1}$ , which is well below the cutoff momentum. The plasmon shows up as a peak in the liquid at an energy loss of 2 eV. The inset shows the elastic scattering peaks and the energy resolution.

scattering in the liquid. There is clearly an additional feature in the mixture at an energy loss of about 2 eV, which is approximately the energy expected for the plasmon in lithium ammonia at this concentration. The inset shows elastic scattering in the sample; the width of the elastic peak was used to determine the experimental resolution. The lower scattering rate in pure ammonia is due to the higher absorption.

Figure 2 shows the behavior of the plasmon as a function of momentum transfer. The plasmon clearly moves to higher energy as the momentum transfer is increased. In addition, both the peak width and the area under the peak increase as  $q$  increases. The plasmon broadens out at the highest momentum transfers and becomes difficult to distinguish from the background. The background was subtracted and the remaining peak was fit to a Lorentzian. At momentum transfers above  $0.7 \text{ \AA}^{-1}$  it becomes difficult to accurately separate the plasmon from the background and so we do not treat these data.

Figure 3(a) shows the plasmon dispersion; the plasmon energy increases for increasing momentum transfer. Figure 3(b) shows the plasmon width (corrected for instrumental resolution), which is finite at  $q = 0$  and strongly increases as a function of momentum transfer.

As a first approximation we compare our results to jellium, that is, a uniform electron gas in a smeared positive background. We use an electron concentration equal to the number of unbound electrons. In this model we treat the electron interactions using the random phase approximation (RPA) which replaces the actual electronic interaction with an average interaction due to all the electrons. The RPA becomes exact as  $q_s$  and  $r_s \rightarrow 0$  and allows an exact computation of  $\varepsilon(\mathbf{q}, \omega)$ .

The plasmon energy at zero momentum transfer is

$$E(0) = \hbar\omega_p = \hbar\left(\frac{4\pi ne^2}{\varepsilon m}\right)^{1/2}, \quad (3)$$

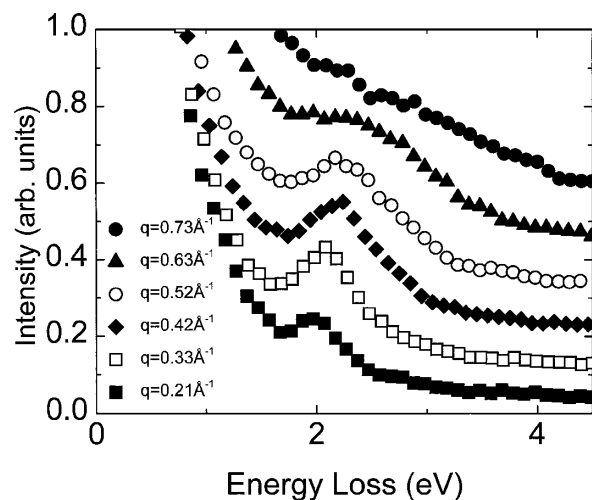


FIG. 2. The momentum dependence of the plasmon. Statistical errors are approximately the size of the symbols. The plasmon displays a positive dispersion, and broadens significantly at higher momenta.

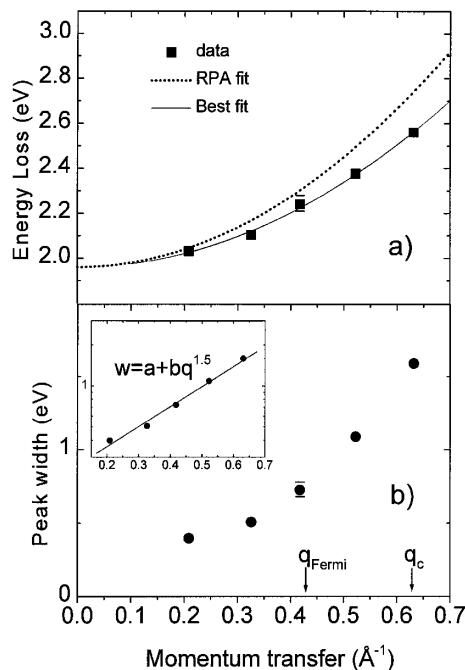


FIG. 3. (a) Dispersion of the plasmon energy. The solid squares are the data, the solid line is the best fit to a quadratic dispersion, and the dotted line is the RPA fit described in the text. (b) Plasmon width as a function of momentum transfer. The inset shows the functional dependence is close to  $q^{1.5}$ .

where  $\omega_p$  is the plasma frequency and  $m$  is the electron mass. For momentum transfer  $q < q_c$  RPA predicts the plasmon dispersion relationship

$$E(q) = E(0) + \frac{\hbar^2}{m} \alpha q^2, \quad (4)$$

where  $\alpha$  is a coefficient that depends only on the electron density.

The plasmon data were fit to a function of the form of Eq. (4). The best fit yields  $E(0) = 1.96 \pm 0.04$  eV and a quadratic dispersion coefficient  $\alpha = 0.33 \pm 0.02$ . For this electron density RPA predicts  $E(0) = 2.2$  eV, if we assume that  $\epsilon$  is 1 [see Eq. (3)]. However, the reduction in  $E(0)$  may be due to polarizability of the lithium ion cores and the ammonia molecules. Assuming  $\epsilon = 1.21$  makes the RPA value for  $E(0)$  match the measured value. This value of  $\epsilon$  changes  $r_s$  from 7.35 to 6 [see Eq. (1)]. It also increases the RPA dispersion coefficient, yielding  $\alpha_{\text{RPA}} = 0.42$ ; the RPA prediction is shown in the figure. As can be seen, the measured dispersion is reduced from the RPA value.

RPA predicts zero linewidth for  $q$  less than some cutoff momentum [9]  $q_c \approx \omega_p/v_F \sim 0.63 \text{ \AA}^{-1}$ , where  $v_F$  is the Fermi velocity. At momenta above  $q_c$ , the plasmon can decay into single electron-hole pairs and has a finite width. However, we do not see evidence for a sharp cutoff, and the plasmon is broad even at  $q \ll q_c$  [see Fig. 3(b)].

There are two ways in which the RPA treatment of the jellium model may be inadequate for this system. First, the RPA does not properly treat electron-electron interac-

tions at large momentum transfers and low densities. In addition, the jellium model does not treat inhomogeneities in the charge distribution, which may also be significant.

We begin by discussing the plasmon dispersion. Many authors have attempted to go beyond the RPA in the jellium model. While the quantitative effects of the electronic interactions vary with the specific model, the interactions always reduce the plasmon dispersion coefficient from the RPA prediction. The RPA with small corrections for the electronic interactions accurately predicts the dispersion of many free electronlike metals, such as Al, Na, and Be [10].

However, some metals such as Li ( $r_s = 3.27$ ) have a measured [11] dispersion ( $\alpha_m = 0.18$ ) significantly less than the RPA prediction ( $\alpha_m = 0.34$ ). In addition, EELS measurements [12] of the plasmon in the heavy alkali metals found the plasmon dispersion to be virtually flat in Rb ( $r_s = 5.2$ ) and even negative in Cs ( $r_s = 5.62$ ). For these values of  $r_s$  theoretical models that use a local field factor to go beyond the RPA predict [13] a positive dispersion, although with a dispersion coefficient reduced from the RPA value. It has been unclear whether these disagreements are due to the insufficiencies in the present theoretical treatment of the electron gas or solid state effects (such as band structure). In contrast to the EELS data, our measured dispersion coefficient at an effective  $r_s = 6$  is positive. While the dispersion coefficient is reduced from the RPA value, the reduction is about a factor of 2 less than has been predicted [13] for this value of  $r_s$ . Since our data show a very different behavior than the heavy alkali metals, this argues that properties not described by the jellium model (such as band structure) must be capable of substantially altering the plasmon properties.

Measurements to determine the effect of band structure on the plasmon were carried out by Schülke and collaborators [14] on single crystals of Li, Be, and Al. They saw virtually no change when they measured the plasmon dispersion along different crystal directions below the cutoff wave vector (although structures at momentum transfers above the cutoff did depend strongly on the crystal orientation). The lower electronic density and lower plasmon energy may make band structure effects more important in this system.

The effect of being a liquid metal is unlikely to be significant. Recent work by Hill *et al.* [11] looked at both the liquid and solid phases of lithium and sodium. Similar studies on Al were carried out by Sternemann *et al.* [15]. The plasmons in the liquid and solid were identical, except for a slight alteration completely attributable to the slightly different densities. Therefore if band structure plays a role in the plasmon dispersion the short-range order in the liquid must result in an effective band structure in the liquid.

Studies of the conduction states by Kohanoff *et al.* [16] suggest that the electronic states in lithium ammonia have a strong  $f$ -symmetry due to the underlying symmetry of the ammonia molecules. As a result, the electrons are not

evenly spread throughout the zone but instead have regions of higher and lower electronic density; this inhomogeneous distribution means that the jellium approximation is an oversimplification. The stiffer dispersion observed here may arise since as we move to larger momentum transfers (and therefore smaller length scales) the local electron density is higher than the average density. A more detailed treatment would require incorporating these effects in RPA.

Next we discuss the linewidth. We assumed that the measured linewidth  $w_m = \sqrt{w_i^2 + w_p^2}$ , where  $w_i$  and  $w_p$  correspond to the instrumental and plasmon linewidths. Treatments of the jellium model to second order in perturbation theory show that the plasmon can decay into two particle-hole pairs below  $q_c$ ; the momentum dependence in this case is  $q^2$ . The calculated width [17] for this decay is smaller by a factor of 20 than our measured data, and we find a momentum dependence [inset in Fig. 3(b)] that is close to  $q^{1.5}$  rather than  $q^2$ .

The failure of the jellium model to explain the width is not unique to this system; all metal plasmons have a finite width at  $q = 0$  that increases with  $q$  even below  $q_c$ . No decay of the plasmon can occur in the jellium model at  $q = 0$ , since no plasmon at finite energy can create a particle-hole pair that conserves energy and momentum. The decay can occur in the presence of a lattice, since the lattice can take up the momentum through an umklapp process. The ratio of the width to the energy at low momentum transfers for  $\text{Li}(\text{NH}_3)_4$  is large, about a factor of 2 greater than in lithium metal [11]. The large width means there must be excitations in the liquid that couple strongly to the plasmons. In lithium ammonia the vibrational excitations of the ammonia molecule may be strongly coupled due to the polarizability of the molecule. Bandlike transitions may also be involved.

In conclusion, we have made the first measurements of the plasmon in the lithium ammonia system, which has the largest  $r_s$  of any metallic system yet measured. We find a plasmon dispersion that is reduced from the RPA value, but by less than has been predicted for a homogeneous electron gas. The plasmon has a large width, indicating numerous decay mechanisms in addition to the two pair particle-hole decay. Future work will concentrate on how the properties of the plasmon evolve as the electron density is changed and studies of the solid phase where reduced elastic scattering will permit measurements at lower energies and larger momentum transfer.

We especially thank Dr. James Dye of Michigan State University for providing very helpful advice on creating the samples. We also thank D. Bortolotti, M. Posada,

and A. Webb for assistance in the laboratory. This work was supported in part by funds from the Faculty Research and Creative Activities Support Fund, Western Michigan University. Measurements were performed at Beamline X21 at the National Synchrotron Light Source, which is supported by the Department of Energy under Contract No. DE-AC02-76CH00016.

- 
- [1] W. Weyl, *Ann. Phys. (Leipzig)* **121**, 606 (1864).
  - [2] See, for instance, G. Lepoutre and M. J. Sienko, *Metal-Ammonia Solutions* (W. A. Benjamin, New York, 1964); J. C. Thompson, *Electrons in Liquid Ammonia* (Oxford University Press, New York, 1976); *Proceedings of Colloque Weyl VI, The Sixth International Conference on Excess Electrons and Metal Ammonia Solutions* [*J. Phys. Chem.* **88**, 3699 (1984)]; *Proceedings of Colloque Weyl VII* [*J. Phys. (Paris)* **1**, C5 (1991)].
  - [3] Zhihong Deng, G. J. Martyna, and M. L. Klein, *Phys. Rev. Lett.* **68**, 2496 (1992), and references therein.
  - [4] Zhihong Deng, G. J. Martyna, and M. L. Klein, *Phys. Rev. Lett.* **71**, 267 (1993).
  - [5] E. D. Isaacs and P. M. Platzman, *Phys. Today* **49**, No. 2, 40 (1996).
  - [6] P. Nozières and D. Pines, *Phys. Rev.* **113**, 1254 (1959).
  - [7] C.-C. Kao, K. Hamalainen, M. Krisch, D. P. Siddons, T. Oversluizen, and J. B. Hastings, *Rev. Sci. Instrum.* **66**, 1699 (1995).
  - [8] P. Abbamonte, Ph.D. thesis, University of Illinois, Urbana-Champaign, 1999 (unpublished).
  - [9] O. Madelung, *Introduction to Solid State Physics* (Springer-Verlag, Berlin, 1981).
  - [10] P. M. Platzman and P. A. Wolff, *Waves and Interactions in Solid State Plasmas* (Academic Press, New York, 1973).
  - [11] J. P. Hill, C.-C. Kao, W. A. C. Caliebe, D. Gibbs, and J. B. Hastings, *Phys. Rev. Lett.* **77**, 3665 (1996).
  - [12] A. vom Felde, J. Fink, Th. Büche, B. Scheerer, and N. Nücker, *Europhys. Lett.* **4**, 1037 (1987); A. vom Felde, J. Sprösser-Prou, and J. Fink, *Phys. Rev. B* **40**, 10181 (1989).
  - [13] P. Vashishta and K. S. Singwi, *Phys. Rev. B* **6**, 875 (1972).
  - [14] W. Schülke, H. Nagasawa, S. Mourikis, and P. Lanzki, *Phys. Rev. B* **33**, 6744 (1986); W. Schülke, H. Nagasawa, S. Mourikis, and A. Kaprolat, *Phys. Rev. B* **40**, 12215 (1989); W. Schülke, H. Schulte-Schrepping, and J. R. Schmitz, *Phys. Rev. B* **47**, 12426 (1993).
  - [15] C. Sternemann, A. Kaprolat, and W. Schülke, *Phys. Rev. B* **57**, 622 (1988).
  - [16] J. Kohanoff, F. Buda, M. Parrinello, and M. L. Klein, *Phys. Rev. Lett.* **73**, 3133 (1994).
  - [17] M. E. Bachlechner, H. M. Böhm, and A. Schinner, *Physica (Amsterdam)* **183B**, 293 (1993).